Stochastic Modeling of Tidal Generation for Transient Stability Analysis: A Case Study based on the All-Island Irish Transmission System

Guðrún Margrét Jónsdóttir and Federico Milano
School of Electrical & Electronic Engineering, University College Dublin, Ireland
gudrun.jonsdottir@ucdconnect.ie, federico.milano@ucd.ie

***Abstract*—The renewable energy currently generated in the Irish system is almost entirely supplied by wind power plants. However, in the sea around Ireland there is a significant tidal energy potential. This paper provides a comparison of these two renewable energy sources, namely wind and tidal, in terms of short-term variability and its impact on the dynamic behavior of the system. With this aim, stochastic models of the short-term variability of these two energy sources are proposed. Simulation results indicate that tidal generation leads to larger frequency variations than those that are caused by wind generation. The paper also shows that the inclusion of frequency control in tidal power plants effectively mitigates such fluctuations.**

***Index Terms*—Irish power system, stochastic differential equations, Stokes wave model, tidal generation, wind generation**

I. Introduction

A. Motivation

Ireland is ideally positioned to capitalize on ocean energy and has claims to one-third of the potential offshore renewable resources in northwestern Europe [1]. A relevant part of such resources is tidal energy. In [2], the tidal resources in Ireland are studied and eleven sites are identified. Although there are multiple techno-economic issues still to be solved [3], the recent success of some tidal generation projects, such as MeyGen (Pentland Firth, Scotland) [4], has demonstrated that tidal stream generation is a viable technology.

Tidal currents have a high long-term predictability compared to other prominent renewable energy sources, e.g. wind and solar [5]. This makes tidal generation an excellent choice for supplying the base load of the system. However, short-term fluctuations (seconds to minutes) in the current are less predictable and can negatively impact the power quality and stability of systems which include tidal generation.

B. Literature review

Uncertainty, introduced through diverse sources, such as loads, wind and solar, can negatively impact the reliability, safety and economy of power systems. The uncertainties in the system can be modeled using Stochastic Differential Equations (SDEs). SDEs are continuous with respect to time and are therefore well equipped to reproduce transient fluctuations in the source of uncertainty. Power system models are typically formalized as a set of Differential-Algebraic Equations (DAEs). This allows for the SDEs to be readily incorporated into the system model and the resulting model is a set of Stochastic Differential-Algebraic Equations (SDAEs).

The use of SDEs for power system studies has been a trending topic over the last few years with the increased uncertainty in the system, introduced with the increasing integration of variable renewable energy sources. In [6], a systematic method to model power systems as SDAEs is presented. The method is demonstrated through a case study of the IEEE 145-bus 50-machine system. A few more studies on multi-bus systems including uncertainties, modeled as SDEs, have been presented in the literature. For example, in [7], the IEEE 145-bus test systems is modified to include wind generation, formulated using SDEs and the systems stability is studied. The Icelandic system is modeled with uncertain variations, modeled as a set of linearized SDEs and its frequency stability assessed in [8] and in [9], the IEEE 39-bus test systems transient stability is studied through SDAEs where wind is modeled as stochastic.

Several SDE-based approaches, on the stochastic modeling of specific energy sources such as wind [10]–[12] and tidal [13], as well as loads [10], [14], have been proposed in the literature. The volatility of wind power is either modeled through the wind power directly, or through the wind speed. In [10], the wind power is modeled based on active power measurements, with a 1 Hz sampling rate, collected in Chile. In this case the wind power is modeled as an exponential function of the Ornstein-Uhlenbeck (OU) process. However, for dynamic studies of the system, modeling the wind speed is to be preferred, as the dynamics associated with the turbine itself can be considered.

In [11] the wind speed is modeled as an exponentially decaying autocorrelated Weibull distributed SDE. However, more detailed models are required to properly capture the autocorrelation of the wind speed. Thus, in [12], a method to build SDEs with an arbitrary probability distribution and autocorrelation is proposed, for wind speed modeling. The method consists in the superposition of OU stochastic processes. This method has since been extended to model the

This material is based upon works supported by the Science Foundation Ireland, under Investigator Programme, Grant No. SFI/15/IA/3074.

short-term variations in tidal current speed [13].

C. Contributions

The contributions of this paper are threefold, as follows.

- Provide a comparison of tidal and wind generation in terms of technology and the uncertainty of the energy source.
- Compare the impact of the short-term uncertainty of tidal and wind generation on the system frequency through a case study of the Irish system. The modeling of the uncertainty of the two energy sources is based on measurements.
- Consider the use of frequency control of the tidal generation to mitigate the effect that waves have on the dynamic behavior of the system.

D. Organization

The remainder of the paper is organized as follows. Section II provides an overview of the current status of tidal generation technology and its similarities to wind generation. Section II also discusses the differences between the variations in the wind speed and the tidal current. Section III outlines the stochastic models used in the case study. In Section IV, the test system and its modeling are presented and simulation results are presented. Finally, in Section V conclusions are drawn and future work is outlined.

II. Tidal Generation

The technology used to harvest the kinetic energy in tidal current is relatively mature compared to other ocean energy technologies. Tidal turbines extract energy from the ocean movement due to the tidal phenomenon. Tides are a consequence of the changing gravitational pull of the sun and moon with respect to the earth's oceans. Tides consists in large bodies of water that move towards and away from the shore. The tidal movement is site specific. Each location experiences diurnal tides (one high, one low in a tidal day), semi-diurnal tides (two high, two low in a tidal day) or a mixture of the two. Tides can be predicted far in advance and with a high degree of accuracy. This fact makes tidal generation one of the more reliable sources of renewable energy and is one of the most relevant reasons for its exploitation.

Numerous types of tidal generation devices have been proposed in the literature. The main research and development focus has been on horizontal-axis tidal stream turbines, with important tidal projects, such as SeaGen in Northern Ireland [15] and more recently MeyGen in Scotland [4] utilizing those. A contributing factor to their dominance is their similarity to wind turbines.

The utilization of similar technology for tidal and wind generation systems is not surprising, as both aim to capture kinetic energy from one kind of a flowing mass. However, several important differences exist between the two energy sources, the density of the flowing mass being one of the most relevant. The density of air is about $1/800$ of the density of water. This means the rated current speed can be much lower, between $2-3$ $\mathrm{m/s}$, compared to the rated wind speed of a wind turbine. Thus, to obtain similar power ratings, the tidal turbine rotor size is much smaller than that of a wind turbine.

Another noticeable difference, when it comes to dynamic analysis, is due to the very input signal, i.e. wind speed and tidal current speed. For its relevance in the case study, the following section is dedicated to this subject.

A. Wind Speed and Tidal Current Speed

If average values over some minutes are considered, the current speed is highly predictable many days or even years in advance. The mean current speed usually has roughly four or eight peaks per day. This is illustrated in Fig. 1.a where an example of measured current speed for Port Mantee, US is shown [16]. Wind power on the other hand will vary with more uncertainty in that minutely to hourly time frame. An example of measured wind speed, collected in Mayo, Ireland, is shown in Fig. 1.b [17].

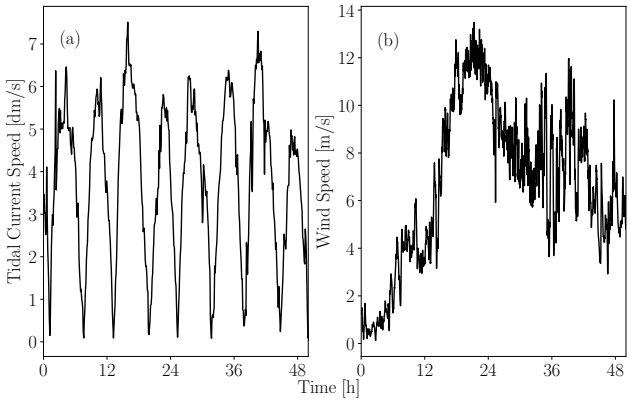

Fig. 1: Wind speed and tidal current speed measurements averaged every 10 minutes [16], [17].

Wind and tidal current speeds are variable on a shorter time scale as well. In the case of wind speed these short-term variations can be due to gusts and/or turbulence. The intensity of the turbulence depends on the terrain surrounding the wind power plant. For a land-based wind turbines, the normal turbulence intensity is close to 20 $\%$ for wind speed of around 12 $\mathrm{m/s}$ [18], while for offshore locations, this percentage is expected to be slightly smaller. An example of measured wind speed, with a sampling frequency of 1 Hz, is shown in Fig. 2.b, measured in Tracy, California [19]. Further details on how these short-term variations in the wind speed are modeled for power system analysis are presented in Section III-B.

Short-term variations in the tidal current are both due to the bottom and side friction and the surface waves. These fluctuations are typically about 10 $\%$ of the mean speed [18]. An example of measured tidal current, with a sampling frequency of 1 Hz, is shown in Fig. 2.a, collected in the European Marine Energy Centre tidal test site in Orkney, UK [20]. In this case the fluctuations are dominated by turbulence.

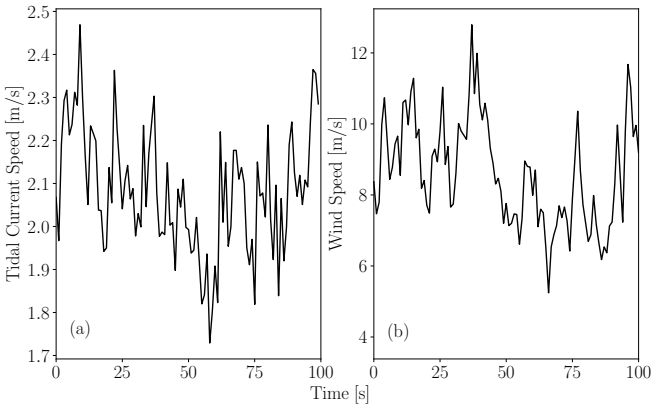

Fig. 2: Wind speed and tidal current speed measurements with a 1 Hz sampling frequency [19], [20].

The tidal current speed can also be subject to wind waves and ocean swells. Wind waves have a relatively short wave length and high frequency. These are caused by local winds. Swells are long wavelength waves that originate in a remote region of the ocean and propagate out of their area of generation. These are considered to have the greatest perturbation effect on the tidal current speed in a tidal turbine, as they travel deep under the ocean surface [21]. Further details on the tidal current models, representing turbulence and wave scenarios, for the case study, are presented in Section III-C.

III. Stochastic Modeling

Traditionally, power systems are modeled as a set of Differential-Algebraic Equations (DAEs). When stochastic perturbations are considered the system model becomes a set of Stochastic Differential-Algebraic Equations (SDAEs), as discussed in [6]. The stochastic processes for these simulations are modeled using Stochastic Differential Equations (SDEs). SDEs have been utilized in previous power systems studies as outlined in Section I-B.

The Ornstein-Uhlenbeck (OU) process is one of the most widely known SDEs because of its simplicity and versatility. The stochastic processes for the simulations presented in the case study are built using OU SDEs. The OU process is a mean reverting Gaussian process. The general form of a SDE defining a OU process is:

$$d\eta(t) = \alpha(\mu - \eta(t))dt + \sigma dW(t), \tag{1}$$

where $\alpha,\ \sigma > 0$ and $W(t)$ is a Wiener process. α is the mean reversion speed of the process, $\eta(t)$, which defines the slope of its exponentially decaying autocorrelation. The process $\eta(t)$ is Gaussian distributed with mean μ and variance $\sigma^2/(2\alpha)$.

The technique proposed in [12] is used to model the stochastic processes with an autocorrelation which is not purely exponentially decaying. It consists in the superposition of OU processes, as defined in (1), to capture the desired autocorrelation. Thus, $\rho(t)$ is a stochastic process defined as the weighted sum of n SDE processes:

$$\rho(t) = \sum_{i=1}^{n} \sqrt{w_i}\,\eta_i(t), \tag{2}$$

where $\eta_i(t)$, with $i \in \{1, \ldots, n\}$, are SDE processes with autocorrelations $R_{\eta_i}(\tau)$, $w_i > 0$ and

$$\sum_{i=1}^{n} w_i = 1. \tag{3}$$

If all n processes have an identical Gaussian probability distribution $\mathcal{N}(\mu_\eta, \sigma_\eta^2)$, the stochastic process $\rho(t)$ has the same Gaussian probability distribution, $\mathcal{N}(\mu_\eta, \sigma_\eta^2)$, and an autocorrelation which is a weighted sum of the autocorrelation functions of the n SDE processes, that is:

$$R_\rho(\tau) = \sum_{i=1}^{n} w_i R_{\eta_i}(\tau). \tag{4}$$

If the n SDE processes in (2) are $\eta(t)$ processes as in (1), the resulting autocorrelation of $\rho(t)$ is a weighted sum of decaying exponential functions and (4) can be rewritten as:

$$R_\rho(\tau) = \sum_{i=1}^{n} w_i \exp(-\alpha_i \tau). \tag{5}$$

Hence, the superposition of SDE processes enables the modeling of any Gaussian stochastic process, with an autocorrelation that can be modeled as a weighted sum of decaying exponentials.

This section provides a quick introduction to the SDEs used in the case study of this paper. The interested reader can find further details on SDEs and the technique above in [12], [22]. The individual stochastic models used to represent the loads, wind speeds and tidal current speeds in the case study are presented next.

A. Load modeling

The stochastic load model considered in this paper is developed based on the well-known voltage dependent load model coupled with OU processes, as follows [6]:

$$\begin{aligned} p_L(t) &= (p_{L0} + \eta_p(t))(v(t)/v_0)^k, \\ q_L(t) &= (q_{L0} + \eta_q(t))(v(t)/v_0)^k, \\ d\eta_p(t) &= \alpha_p(\mu_p - \eta_p(t))dt + \sigma_p dW(t), \\ d\eta_q(t) &= \alpha_q(\mu_q - \eta_q(t))dt + \sigma_q dW(t), \end{aligned} \tag{6}$$

where $p_L(t)$ and $q_L(t)$ are the active and reactive power of the load, respectively, and p_{L0} and q_{L0} are parameters representing active and reactive load powers at $t = 0$. $v(t)$ is the voltage magnitude at the bus where the load is connected and v_0 is the value of this voltage magnitude at $t = 0$.

The model (6) can, through the exponent k define whether the load is a constant power load ($k = 0$), a constant current load ($k = 1$) or a constant impedance load ($k = 2$). The variability is modeled through the stochastic processes $\eta_p(t)$ and $\eta_q(t)$ which are formulated as OU processes, where the

parameters α, μ and σ have the same meaning as in (1). In the case study, the uncertainty is set as 10 % of the nominal load power and the mean reversion speed is set to $\alpha_p = \alpha_q = 0.02$.

B. Wind speed modeling

The wind speed model considered in this paper consists of two parts: a constant mean wind speed, v_c and a Gaussian stochastic process, $\rho_w(t)$. The wind is modeled in this way since the wind speed variations within a 10 minute time frame can be assumed to be Gaussian distributed around a certain mean v_c [23]. The wind speed model used for each wind farm in the Irish system is:

$$v_{wind}(t) = v_c + \rho_w(t), \tag{7}$$

where $v_{wind}(t)$ is the modeled wind speed time-series and $\rho_w(t)$ is a stochastic process as defined in (2). Thus, $\rho_w(t)$ has the probability distribution $\mathcal{N}(\mu_{\rho_w}, \sigma^2_{\rho_w})$ and an autocorrelation as in (5).

The following assumptions are made for the wind farm modeling:

- All wind farms are assumed to be uncorrelated. This is a fair assumption as short-term wind speed fluctuations are uncorrelated for larger distances.
- Wind speed is location dependent. However, since the details of the exact locations of wind generators are not available to the authors, the wind speed, for all locations, is modeled using the same model parameters. The parameters for the autocorrelation are set as shown in Table I based on previous data analysis in [12] of the data set available in [19].
- The standard deviation of the process is set to be 20 % of the mean wind speed v_c as supported by [18] and analysis of the data set in [19].
- The damping effect of the rotor blades is modeled through a low-pass filter as presented in [24]. The time constant, T_b, of the filter is dependent on the radius of the rotor. In the case study, $T_b = 10$ s for all wind power plants as the rotor size of individual turbines is unknown.
- The aggregated wind speed is defined through the σ_{ρ_w} parameter:

$$\sigma_{\rho_w} = 0.2 \cdot v_c / \sqrt{2 n_{turb}}, \tag{8}$$

  where n_{turb} is the number of turbines in the wind farm. Thus, the standard deviation of the modeled wind speed decreases in proportion to the number of turbines, as the variability of wind speed averages out over a spread wind farm.

C. Tidal current speed modeling

The proposed tidal current speed model consists of three parts.

a. The variations in the current due to the tidal phenomenon are very slow and relatively small in the time-frame of seconds to minutes. Thus, the predicted tidal current speed is modeled as a constant, v_{ct}.

TABLE I: The SDE parameters for the wind and tidal current speed models used in the case study.

SDE process	**Parameters**	
Wind speed	$w_1 = 0.35$	$\alpha_1 = -0.3$
	$w_2 = 0.5$	$\alpha_2 = -0.03$
	$w_3 = 0.15$	$\alpha_3 = -0.0001$
Tidal current speed	$w_1 = 0.23$	$\alpha_1 = -5$
	$w_2 = 0.32$	$\alpha_2 = -0.2$
	$w_3 = 0.45$	$\alpha_3 = -0.04$

b. The stochastic turbulence, $\rho_t(t)$, in the current speed is modeled using a stochastic process as defined in (2). It is defined in the same way as for the wind speed (see Section III-B). The only difference is that the standard deviation of the tidal current speed is set to be 10 % of the current speed, v_{ct}, and the autocorrelation parameters are set based on data analysis in [13][1]. The parameters are shown in Table I.

c. The third part represents the effect of waves on the tidal current, $v_{\text{waves}}(t)$.

The resulting tidal current speed model is the following:

$$v_{\text{tide}}(t) = v_{\text{ct}} + \rho_t(t) + v_{\text{waves}}(t). \tag{9}$$

The ocean sea state is affected by a range of waves at the same time. These waves are generally modeled using the first order Stokes model representing a random sea-state [25]:

$$v_{\text{waves}}(t) = \sum_{i=1}^{N} a_i \omega_i \frac{\cosh[k_i(h+d)]}{\sinh(k_i d)} \cos[\omega_i t - k_i x + \phi_i], \tag{10}$$

where h is the vertical distance from the sea surface to the hub height of the tidal turbine, positive upwards, and d is the sea depth. ϕ_i are random phases, uniformly distributed between 0 and 2π, ω_i is the frequency of the i-th frequency component, k_i is the wave number of the i-th frequency component. Finally

$$a_i = \sqrt{2 S(\omega_i) \Delta\omega_i} \tag{11}$$

is the amplitude of the i-th frequency component, defined from the frequency spectrum, $S(\omega)$, of the waves.

The frequency spectrum considered in this paper is the JONSWAP spectrum [25]. The wave angular frequency, ω_i, is within the frequency band, $\Delta\omega_i$, and N different frequency components are considered to represent the random sea-state. The JONSWAP spectrum is defined as:

$$S(\omega) = \frac{m g^2}{\omega^5} \exp\left(-1.25 \left(\frac{\omega_p}{\omega} \right)^4 \right) \gamma^Y, \tag{12}$$

where g is the acceleration due to gravity, ω_p is the peak frequency of the spectrum and γ is the peak enhancement factor which controls the sharpness of the peak. m is the

[1]Both the wind and tidal current speed model parameters are set based on measured data, where the fluctuations have been separated from the rolling average of the data, over a 10 minute time frame.

intensity of the spectrum and can be defined for North Sea applications [25] as:

$$m = 5.058\left(\frac{H_s}{T_p^2}\right)^2 (1 - 0.287\ln\gamma), \tag{13}$$

where H_s is the significant wave height, $T_p = 2\pi/\omega_p$ is the peak wave period.

Waves can be thought of as an intermittent disturbance. They are not always present and are not likely to effect the different locations at the same time, with the same intensity. Thus, the Stokes model, coupled with the JONSWAP spectrum, is set to represent different wave scenarios, as discussed in Section IV-C.

Note that to take into account the aggregation of the full tidal farm in each location the aggregation model for the wave component of the tidal current, presented in [26] is utilized.

IV. Case Study

A. All-Island Irish Transmission System

The Irish system is a relatively-small isolated transmission system. It consists of two separate 50 Hz grids which are AC interconnected and operated by independent TSOs: System Operator for Northern Ireland (SONI) and Eirgrid Group. The current transmission peak of the system is about $5,500$ MW and the demand is forecasted to grow between 22 % and 53 % by 2030 [27]. The system has two HVDC interconnections, to Scotland and Wales, both with a capacity of 500 MW, flowing in both directions.

The installed wind generation has been rapidly increasing over the last 10 years. At present, the record of produced wind power in the Irish system is approximately $3,500$ MW and the system is able to handle upto 65 % renewable energy, primarily composed of wind power [28].

Ireland had the world's first large scale commercial tidal stream generators in operation from 2003 until 2017. Those turbines were a part of the SeaGen tidal test project and were located in Northern Ireland's Strangford Lough, producing 1.2 MW [15]. This project has provided valuable information for further development of tidal generation in Irish waters and has shown that tidal generation is a viable energy source for the Irish system. In [2], Ireland's tidal resources were assessed. Eleven practical resource sites for tidal generation were identified. The four sites with the greatest estimated capacity are shown in Fig. 3. Table II shows the potential energy of the four locations.

TABLE II: The potential energy and installed power at the four modeled tidal power locations [2].

Location	Name	Potential Energy [GWh/y]	Installed Power [MW]
1	Inishtrahull Sound	514	67
2	Shannon Estuary	367	34
3	Tuskar Rock	420	47
4	Codling	791	69

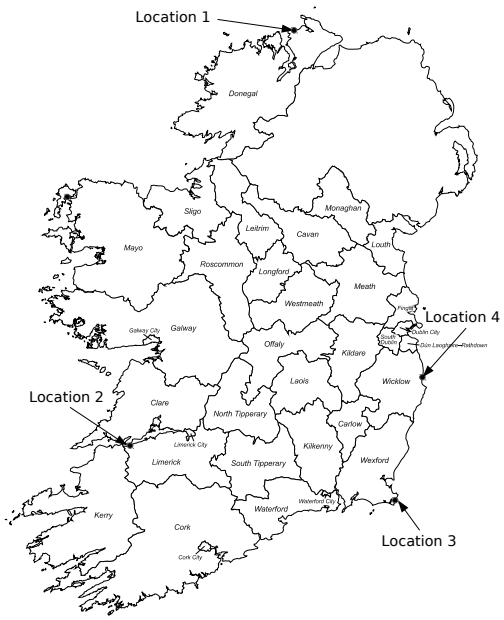

Fig. 3: The top four locations of potential tidal generation as identified in [2].

B. System Model

The Irish transmission system model used for this case study consists of $1,479$ buses, $1,851$ transmission lines and transformers, 245 loads, 22 conventional synchronous power plants, modeled with 6th order synchronous machine models, with AVRs and turbine governors, 6 PSSs, and 169 wind power plants, of which 159 are DFIGs and 10 are CSWTs. In the system for this case study the total load of the system is $2,215$ MW and 25 % of the total generated power is supplied by wind.

The tidal power plants are assumed to be installed in the four locations shown in Fig. 3. The combined generation of these four locations is set to be 10 % of the total generation in the system. The local wind generation in each location is substituted with tidal generation. The set power of the tidal generation at each location is based on their potential energy and is shown in Table II.

The system is modeled as a set of SDAEs where the loads, wind and tidal generation are modeled using SDEs, as presented in Section III. All simulations were carried out using Dome, a Python-based software tool for power system analysis [29]. Dome solves the SDEs using the Itô integral. It supports solving the SDEs using either the Euler-Maruyama or Milstein integration method. For this case study the Euler-Maruyama is used [22].

C. Scenarios

Five scenarios for the Irish power system model are studied:

- **Scenario 1:** The load is stochastic and modeled as presented in Section III-A. This serves as a base scenario. Thus, the same stochastic load models are used in the remaining scenarios.

- **Scenario 2:** The onshore wind, 25 % of generation, is stochastic, modeled as presented in Section III-B.
- **Scenario 3:** Stochastic onshore wind, 15 % of generation, and stochastic offshore wind, 10 % of generation.
- **Scenario 4:** Stochastic onshore wind, 15 % of generation, and stochastic tidal, 10 % of generation, modeled as presented in Section III-C, without waves.
- **Scenario 5:** Same as Scenario 4, that is stochastic onshore wind, 15 % of generation, and stochastic tidal, 10 % of generation, but the tidal generation is disturbed by waves.

In Scenario 3 - 5 offshore wind and tidal generation has been installed in the locations identified in Fig. 3, replacing 10 % of the local onshore wind generation.

Scenario 5 includes three cases, where waves effect the tidal current, presented in Table IV. Typically, the sea surface is assumed to be stationary for 20 minutes, upto a couple of hours. A stationary sea-state can be characterized by a set of parameters. These are the significant wave height, H_s, and the peak wave period, T_p. The significant wave height is defined as the mean wave height (trough to crest) of the highest third of the waves. The peak wave period is the wave period with the highest energy. The wave parameters for the considered sea-states are based on those listed in Table 3.17 in [25]. The parameters utilized for different sea-states in the case study are shown in Table III, where H_s refers to the significant wave height and T_p to the peak wave period; and $T_{\min} - T_{\max}$ gives the range of wave periods, sampled from the JONSWAP spectrum in (12), for the Stokes wave model in (10).

TABLE III: The three sea-states considered for Scenario 5.

Sea-state	H_s [m]	T_p [s]	$T_{\min} - T_{\max}$ [s]
(S) Small waves	1	5	$1.4 - 8.8$
(M) Moderate waves	2.5	7	$2.8 - 13.5$
(L) Large waves	5	10	$3.8 - 15.5$

The three cases for Scenario 5 shown in Table III also take into account the locations of the four tidal power plants. The largest significant wave heights, of about 5 meters, are seen on the west coast during winter. On the other hand, the average significant wave heights, in the Irish sea, do not exceed 2 meters, during any season [30]. Thus, Location 1 & 2 are more likely to experience higher significant wave heights than Location 3 & 4, as they are facing the Atlantic ocean. Specifically, Location 1 is likely to experience the worst wave conditions. Table IV shows the sea-state at each location, for the three cases of Scenario 5.

TABLE IV: The sea-state at each location, for the three cases considered for Scenario 5.

Case\Location	1	2	3	4
a	S	S	S	S
b	M	M	S	S
c	L	M	S	S

The ramp rates of the Center of Inertia (COI) frequency are utilized to compare the scenarios. Ramp rates are computed as:

$$\Delta_h x_t = x_t - x_{t-h} \tag{14}$$

for time lags $h = 0 - 100$ s, where x_t is the COI frequency at time t. Then, the standard deviation of the ramp rates, $\Delta_h x_t$, for each time step h is computed.

D. Wind vs Tidal

The Irish system with all the loads modeled as stochastic (Scenario 1), as presented in Section III-A, is studied first. This scenario serves as a reference for the remaining scenarios. To validate the stochastic load scenario, frequency data from the Irish system, gathered in the AMPSAS project is used. The frequency is measured with a 10 Hz sampling frequency. In this case, the morning of a singular day, that is the 20th of May in 2014, is considered. During this time period there was almost no wind generation, hence the stochastic fluctuations in the frequency are mainly due to loads, as well as dispatches. Further details on these measurements are provided in [31].

Fig. 4 shows the standard deviation of the ramp rates of the measured frequency data and the COI frequency, for the simulated Scenario 1. The model underestimates the frequency ramps in the initial 20 s, when compared to the measured data. However, for higher time steps, the model, for Scenario 1, and the measured data are in agreement.

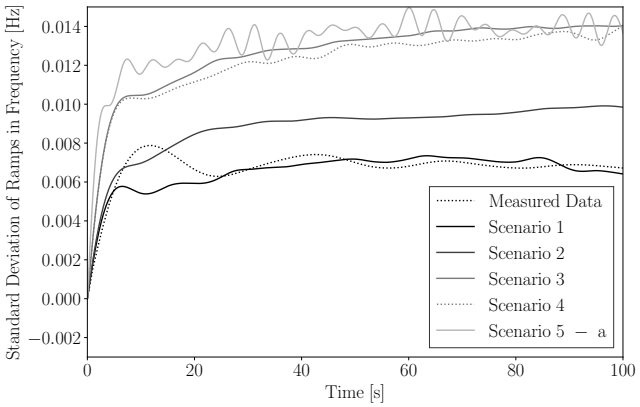

Fig. 4: The standard deviation of the ramps in the frequency of the COI for Scenario 1-5, as well as of the measured frequency [31]. Ramp rates are computed as in (14).

The five different scenarios, as presented in Section IV-C, are compared in Fig. 4. The inclusion of stochastic wind, in Scenario 2, increases the standard deviation of the ramp rates by approximately 25 %. An even bigger change is seen for Scenario 3-5. For these scenarios, however, the generation profile of the system had to be modified to accommodate offshore wind or tidal power plants.

The wind generation in Ireland is mostly composed of small farms spread across the system. For Scenario 3-5, these small farms are replaced by four much larger offshore wind or tidal farm. This causes relatively larger power fluctuations to be introduced in four points in the system. Whereas, for Scenario 2, smaller power fluctuations are installed in locations spread across the area.

Fig. 4 shows that Scenario 4 has slightly smaller frequency variations than Scenario 3. This indicates that offshore wind

would introduce larger frequency variations than tidal generation. However, the set up of the farms, the number of turbines and the turbine sizes also impact the stochastic variations in the output power of the farm. Thus, it cannot be claimed that either source introduces less frequency variations. It can only be stated that tidal generation, when compared to wind generation, if no waves are presents, does not necessarily introduce bigger system frequency variations.

The trajectories of the standard deviation of the frequency ramps for Scenario 5-a are shown in Fig. 4. In this case, all tidal farms are subject to relatively small waves simultaneously. This is the most common wave scenario for the Irish system. The inclusion of waves in the tidal current results in oscillatory fluctuations in the power outputs of the tidal farms, with a time period of less than 10 seconds. This increases the frequency variability, for the initial 20 seconds and introduces oscillations in the system frequency.

Scenario 5-b represents moderate waves in both Location 1 & 2, which are facing the Atlantic ocean. In this case, frequency ramps have a standard deviation of about 0.015 Hz, within a few seconds, as shown in Fig. 5. This state is likely to last for 20 minutes upto a few hours at a time.

Scenario 5-c represents the worst case scenario. In this case Location 1 is experiencing large waves, with longer time periods, that is swell waves. This case is characterized by unacceptable frequency variations. Energy storage systems can be installed along side tidal generation, as suggested in [21] to mitigate these fluctuations. An alternative solution is to include primary frequency control in the tidal generation as discussed in the next section.

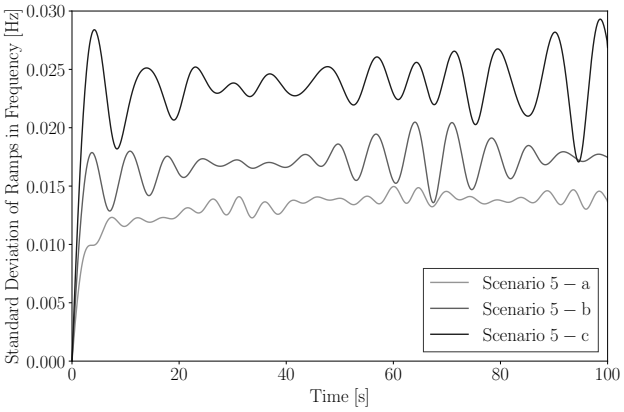

Fig. 5: The standard deviation of the ramps in the frequency of the COI for Scenario 5, case a, b and c. Ramp rates are computed as in (14).

E. Frequency control of tidal generation

In this section, frequency control of tidal generation is considered, to reduce the frequency variability caused by the waves of Scenario 5-c. The similarity between tidal and wind turbines allows for the the frequency control implemented for wind turbines to be adapted for tidal turbines. A common approach for wind turbine frequency control is to bypass the Maximum Power Point Tracking (MPPT) and set the power output based on the deviation of the measured frequency (droop control) and/or Rate of Change of Frequency (ROCOF) control. The combination of the two strategies proposed in [32] for wind turbines is considered below.

The droop controller, with gain $1/R$, is comparable to the primary frequency controller of a synchronous machine. The ROCOF controller consists of a low-pass filter with time constant T_l, the time derivative of the frequency measurement and a gain K_l. The two controllers are complementary. The ROCOF control is faster and has its main effect in the very first instants after the frequency drop. However, the droop control is slower and mitigates the frequency deviation [32].

Fig. 6 shows the comparison of the three different cases for Scenario 5 with the inclusion of frequency control in the four tidal power plants. Compared to the results presented in Fig. 5, frequency variations are approximately halved in size for all three cases. For comparison, Fig. 6 also shows Scenario 2 and 3, i.e. the two scenarios with only wind generation. The frequency control of the tidal turbines effectively mitigates the frequency variations for both Scenario 5-a and 5-b to be less than those for Scenario 3, excluding the first few seconds. Therefore, coupling frequency control to tidal generation can reduce the frequency variations, due to the waves, to an acceptable level.

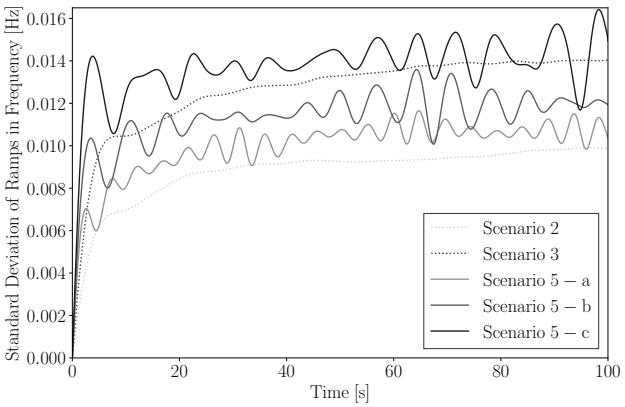

Fig. 6: Standard deviation of the ramps in the frequency of the COI for Scenario 5, case a, b and c with frequency control. Scenarios 2 and 3 are shown for comparison. Ramp rates are computed as in (14).

As a final remark, it is important to note that the sea state is strongly dependent on the location, as discussed in Section IV-C. Thus, the location is the first design parameter to be considered to reduce the impact of waves on tidal generation. If the potential tidal locations are all prone to extreme wave conditions, it is key to determine the optimal placement for the tidal power plants to minimize the impact of waves on the system. In the case of the Irish system, for Location 1 and 2, Scenario 5-c represents the worst case scenario, while for Location 3 and 4 the frequency variations due to wave disturbance would not get bigger than those shown for Scenario 5-a. Thus, it appears sensible to commission tidal installments on the east coast first, e.g. Locations 3 and 4.

V. Conclusions

This paper discusses the frequency fluctuations of the Irish system due to wind and/or tidal generation for different scenarios. Simulation results indicate that tidal generation does not introduce higher frequency variations than wind, except when waves are present in the tidal current. In that case, the output of the tidal generation fluctuates periodically, which results in significant fluctuations of the frequency of the system. The paper also shows the such frequency fluctuations can be mitigated by including proper frequency control in the tidal turbines.

Future work will focus on other renewable energy sources for the Irish system, such as generation based on wave energy, and compare their dynamic modeling and impact on the grid with respect to offshore wind and tidal generation.

References

[1] E. Robinson and D. McDonnell, "Ireland's potential role in the development of offshore renewables: Operations and maintenance," *Engineers Journal*, May 1, 2018.

[2] F. O'Rourke, F. Boyle, and A. Reynolds, "Tidal current energy resource assessment in Ireland: Current status and future update," *Renewable and Sustainable Energy Reviews*, vol. 14, no. 9, pp. 3206–3212, 2010.

[3] E. Segura, R. Morales, J. Somolinos, and A. López, "Techno-economic challenges of tidal energy conversion systems: Current status and trends," *Renewable and Sustainable Energy Reviews*, vol. 77, pp. 536–550, 2017.

[4] L. Buchsbaum, "MeyGen Array Sets Global Record for Harnessing Tidal Power," September 2018. [Online]. Available: https://www.powermag.com/meygen-array-sets-global-records-for-harnessing-tidal-power/ [Accessed in September 2019]

[5] J. Widén, N. Carpman, V. Castellucci, D. Lingfors, J. Olauson, F. Remouit, M. Bergkvist, M. Grabbe, and R. Waters, "Variability assessment and forecasting of renewables: A review for solar, wind, wave and tidal resources," *Renewable and Sustainable Energy Reviews*, vol. 44, pp. 356–375, 2015.

[6] F. Milano and R. Zárate-Miñano, "A systematic method to model power systems as stochastic differential algebraic equations," *IEEE Transactions on Power Systems*, vol. 28, no. 4, pp. 4537–4544, 2013.

[7] B. Yuan, M. Zhou, G. Li, and X.-P. Zhang, "Stochastic small-signal stability of power systems with wind power generation," *IEEE Transactions on Power Systems*, vol. 30, no. 4, pp. 1680–1689, 2014.

[8] H. Li *et al.*, "Analytic analysis for dynamic system frequency in power systems under uncertain variability," *IEEE Transactions on Power Systems*, vol. 34, no. 2, pp. 982–993, 2018.

[9] W. Wu, K. Wang, G. Li, and Y. Hu, "A stochastic model for power system transient stability with wind power," in *IEEE PES General Meeting, Washington*, 2014.

[10] H. Verdejo, A. Awerkin, W. Kliemann, and C. Becker, "Modelling uncertainties in electrical power systems with stochastic differential equations," *International Journal of Electrical Power & Energy Systems*, vol. 113, pp. 322–332, 2019.

[11] R. Zárate-Miñano, M. Anghel, and F. Milano, "Continuous wind speed models based on stochastic differential equations," *Applied Energy*, vol. 104, pp. 42–49, 2013.

[12] G. M. Jónsdóttir and F. Milano, "Data-based continuous wind speed models with arbitrary probability distribution and autocorrelation," *Renwable Energy*, vol. 143, pp. 368–376, 2019.

[13] ——, "Modeling of short-term tidal power fluctuations," *IEEE Transactions on Sustainable Energy*, 2019.

[14] K. Wang and M. L. Crow, "Numerical simulation of stochastic differential algebraic equations for power system transient stability with random loads," *IEEE PES General Meeting, Detroit*, 2011.

[15] G. Savidge *et al.*, "Strangford Lough and the SeaGen tidal turbine," in *Marine renewable energy technology and environmental interactions*. Springer, 2014, pp. 153–172.

[16] NOAA - Tides and currents, "Current data, February 15, 2019." [Online]. Available: https://tidesandcurrents.noaa.gov/cdata/ [Accessed in May 2019]

[17] Met Éireann, "The Irish meterological service online, historical data," 2019. [Online]. Available: https://www.met.ie/climate/available-data/historical-data/ [Accessed in May 2019]

[18] A. I. Winter, "Differences in fundamental design drivers for wind and tidal turbines," in *IEEE OCEANS, Spain*, 2011.

[19] RE<C: Renewable Electricity Less Than Coal, "Surface Level Wind Data Collection," 2011. [Online]. Available: https://code.google.com/archive/p/google-rec-csp/ [Accessed in March 2019]

[20] The Reliable Data Acquisition Platform for Tidal energy (ReDAPT), "Met-Ocean Data Science for Offshore Renewable Energy Applications)," 2017. [Online]. Available: http://redapt.eng.ed.ac.uk/index.php [Accessed in February 2019]

[21] Z. Zhou, M. Benbouzid, J. F. Charpentier, F. Scuiller, and T. Tang, "A review of energy storage technologies for marine current energy systems," *Renewable and Sustainable Energy Reviews*, vol. 18, pp. 390–400, 2013.

[22] P. E. Kloeden, E. Platen, and H. Schurz, *Numerical solution of SDE through computer experiments*. Springer Science & Business Media, 2012.

[23] B. C. Cochran, "The influence of atmospheric turbulence on the kinetic energy available during small wind turbine power performance testing," *Ceder-Ciemat. Spain April*, 2002.

[24] T. Petru and T. Thiringer, "Modeling of wind turbines for power system studies," *IEEE Transactions on Power Systems*, vol. 17, no. 4, pp. 1132–1139, 2002.

[25] S. Chakrabarti, *Handbook of Offshore Engineering (2-volume set)*. Elsevier, 2005.

[26] A. N. Einrí, G. M. Jónsdóttir, and F. Milano, "Modeling and control of marine current turbines and energy storage systems," *IFAC-PapersOnLine*, vol. 52, no. 4, pp. 425–430, 2019.

[27] EirGrid Group, "All-Island Generation Capacity Statement 2018-2027," 2018. [Online]. Available: http://www.eirgridgroup.com/site-files/library/EirGrid/Generation_Capacity_Statement_2018.pdf [Accessed in September 2019]

[28] ——, "EirGrid Group achieves record level of variable renewable energy on Irish electricity system," April 13, 2018. [Online]. Available: http://www.eirgridgroup.com/newsroom/record-renewable-energy-o/ [Accessed in September 2019]

[29] F. Milano, "A Python-based software tool for power system analysis," *IEEE PES General Meeting, Vancouver*, 2013.

[30] S. Gallagher, R. Tiron, and F. Dias, "A long-term nearshore wave hindcast for Ireland: Atlantic and Irish Sea coasts (1979–2012)," *Ocean Dynamics*, vol. 64, no. 8, pp. 1163–1180, 2014.

[31] M. Adeen, G. M. Jónsdóttir, and F. Milano, "Statistical correlation between wind penetration and grid frequency variations in the irish network," in *IEEE International Conference on Environment and Electrical Engineering*, 2019.

[32] J. Cerqueira *et al.*, "Comparison of the dynamic response of wind turbine primary frequency controllers," in *IEEE PES General Meeting, Chicago*, 2017.